



OPEN ACCESS

EDITED BY

Fernanda Visioli,
Federal University of Rio Grande do Sul, Brazil

REVIEWED BY

Vito Carlo Alberto Caponio,
University of Foggia, Italy
Gaurisankar Sa,
Bose Institute, India
Mazin Mohammed,
University of Anbar, Iraq

*CORRESPONDENCE

Shichao Li
✉ lishichao221@gmail.com
Fanglei Ye
✉ fccyefl@zzu.edu.cn
Le Wang
✉ fccwangl22@zzu.edu.cn

†These authors have contributed equally to this work

RECEIVED 25 October 2024

ACCEPTED 17 January 2025

PUBLISHED 07 February 2025

CITATION

Zhang Y, Wang Y, Peng J, Zhao K, Li L, Zhang Y, Zhai Z, Yuan S, Li S, Ye F and Wang L (2025) Expression and prognostic significance of the m6A RNA methylation regulator HNRNPC in HNSCC. *Front. Oncol.* 15:1516867. doi: 10.3389/fonc.2025.1516867

COPYRIGHT

© 2025 Zhang, Wang, Peng, Zhao, Li, Zhang, Zhai, Yuan, Li, Ye and Wang. This is an open-access article distributed under the terms of the [Creative Commons Attribution License \(CC BY\)](https://creativecommons.org/licenses/by/4.0/). The use, distribution or reproduction in other forums is permitted, provided the original author(s) and the copyright owner(s) are credited and that the original publication in this journal is cited, in accordance with accepted academic practice. No use, distribution or reproduction is permitted which does not comply with these terms.

Expression and prognostic significance of the m6A RNA methylation regulator HNRNPC in HNSCC

Yulin Zhang^{1†}, Yixu Wang^{2†}, Jilin Peng¹, Kun Zhao¹, Ling Li¹, Yuan Zhang¹, Ziyu Zhai¹, Sijie Yuan¹, Shichao Li^{3,4,5*}, Fanglei Ye^{1*} and Le Wang^{1*}

¹Department of Otolaryngology Head and Neck Surgery, The First Affiliated Hospital of Zhengzhou University, Zhengzhou, China, ²Department of Otolaryngology, Head and Neck Surgery, People's Hospital, Peking University, Beijing, China, ³Department of Otolaryngology Head and Neck Surgery, Henan Provincial People's Hospital, Zhengzhou, Henan, China, ⁴Department of Otolaryngology Head and Neck Surgery, People's Hospital of Zhengzhou University, Zhengzhou, Henan, China, ⁵Department of Otolaryngology Head and Neck Surgery, People's Hospital of Henan University, Zhengzhou, Henan, China

Background: N6-methyladenosine (m6A) RNA modification is crucial for tumor development and progression; however, which m6A regulators play a pivotal role in head and neck squamous cell carcinoma (HNSCC) remains ambiguous.

Methods: Utilizing the Cancer Genome Atlas (TCGA) database, the expression levels of m6A regulators in HNSCC were examined, which led to the identification of heterogeneous nuclear ribonucleoprotein C (*HNRNPC*) as a key gene. Further experiments were performed in patient samples, stable cell lines, and a murine xenograft tumor model.

Results: A reliable survival risk model of m6A was constructed based on the TCGA database. Gene Expression Omnibus (GEO), normal and tumor tissue microarrays (TMA), and tumor tissue samples from patients with HNSCC were observed that a high level of *HNRNPC* expression was closely linked to a poor prognosis among patients. Knockdown of *HNRNPC* in the HNSCC cell lines HSC-3 and CAL-27 resulted in a significant decrease in proliferation, invasion, and malignant transformation abilities. RNA sequencing (RNA-seq) and methylated RNA immunoprecipitation and sequencing (MeRIP-seq) data revealed that *HNRNPC* is involved in cell differentiation, cell migration and apoptosis. The mouse xenograft model elucidated that *HNRNPC* can promote tumorigenesis and progression of HNSCC.

Conclusions: *HNRNPC* can serve as a valuable predictor of tumor progression and prognosis in patients with HNSCC.

KEYWORDS

heterogeneous nuclear ribonucleoprotein C, head and neck squamous cell carcinoma, prognostic significance, tumor progression, N6-methyladenosine

Introduction

Head and neck squamous cell carcinoma (HNSCC) arises in the oropharynx, larynx, oral cavity, and hypopharynx and is the sixth most frequent type of malignant tumor worldwide (1). Patients are often diagnosed with advanced disease, which is more challenging to manage and may even be incurable. As a result, aggressive treatment options are often required, which can impact quality of life and may leave the patient functionally disabled (2). Despite significant advancements in treatment strategies over the past few decades (3), encompassing innovations in surgical procedures, radiation therapy, and cytotoxic drug therapies, recurrence and nodal metastasis persist in greater than 50% of HNSCC patients, emphasizing the low 5-year survival rate (1). Accurate prognostic assessment is therefore fundamentally important for the successful clinical management and shaping of personalized treatment choices for HNSCC.

N6-methyladenosine (m6A), methylation at the N6 position of adenosine, is the most prevalent modification in eukaryotes (4). The process of m6A modification is reversible (5) and consists of “writers” (METTL3, METTL14, and WTAP) with methyltransferase activity (6), “erasers” (FTO and ALKBH5) with demethyltransferase activity (7), and “readers” (YTHDC2, IGF2BP2, and HNRNPC) with methylation recognition function (8). The roles of m6A in the pathogenesis and progression of cancer have been confirmed in recent years (9). HNRNPC has been reported as the most common RNA binding protein (10) and one member of the m6A reader protein family (11), participating in RNA splicing (12), sequence-unspecific RNA exportation (13), RNA expression, RNA stability (14), RNA 3' end processing (15), and translation (16). Increasing evidence highlights the aberrant upregulation of HNRNPC in a variety of tumors, which plays a non-negligible role in tumorigenesis and progression and affects overall survival in glioblastoma (17), hepatocellular carcinoma (18) and breast cancer (19). Despite extensive research and the analysis of innumerable HNRNPC profiles derived from cancer cells, the precise clinical prognostic significance of HNRNPC in HNSCC and its potential physiological functions within tumor cells are yet to be definitively understood. At present, there exists no comprehensive investigation on the role of HNRNPC in HNSCC.

We created a survival risk model using m6A-associated protein expression from the TCGA HNSCC dataset, and validated it with GEO database. Along with clinical HNSCC samples, showed that *HNRNPC* had the most noticeable difference in expression between tumor and normal samples. Knocking down *HNRNPC* in HNSCC cell lines HSC-3 and CAL-27 led to significant reductions in cell proliferation, invasion, and tumorigenesis. RNA-seq and MeRIP-seq data supported our findings, emphasizing the crucial role of HNRNPC in promoting malignant behavior in HNSCC cells. Targeting HNRNPC could potentially inhibit these cellular processes, offering a new avenue for improving patient prognosis and treatment outcomes.

Materials and methods

Patient samples

We selected 150 patients with head and neck squamous cell carcinoma (HNSCC) from the Department of Head and Neck Surgery and Stomatology at the First Affiliated Hospital of Zhengzhou University. Tissues removed during surgery were examined to confirm the diagnosis. The clinicopathological characteristics are shown in Table 1. Formalin-fixed and paraffin embedded (FFPE) tissues were used for qPCR and immunohistochemistry. Normal and tumor tissue microarrays (TMAs) were purchased from Servicebio Technology Co., Ltd., (Wuhan, China) which contained 45 cases of squamous carcinoma and 45 normal tissue samples. The present study was approved by the Ethics Committee of the First Affiliated Hospital of Zhengzhou University. Informed consent was waived due to the retrospective nature of tissue sample collection from patients diagnosed with HNSCC. Additionally, there exist no personal privacy or commercial interests.

Public mRNA expression datasets

RNA-seq data for HNSCC and normal samples were downloaded from the TCGA database. Level 3 TCGA RNA-seq data for 517 HNSCC samples (Illumina[®] HiSeq 2000), with clinical annotations and overall survival (OS) information acquired from the Cancer Genomics Browser of University of California Santa Cruz (UCSC) (<https://genomecancer.ucsc.edu>), were used as the training set. A total of 253 primary cases, also with clinical annotations and OS information, were selected from the GSE65858 dataset (<http://www.ncbi.nlm.nih.gov/geo>).

Cell culture

The HNSCC cell lines CAL-27 and HSC-3 were purchased from the Chinese Academy of Sciences typical culture preservation committee cell bank. Cells were maintained in Dulbecco's modified Eagle's medium (DMEM) (high glucose; Gibco) supplemented with 10% fetal bovine serum (FBS), 100 U/mL penicillin, and 100 mg/mL streptomycin (Invitrogen, Grand Island, NY, USA) and cultured in a humidified atmosphere of 5% CO₂ at 37°C.

ShRNA lentivirus production and infection

HEK293T cells were co-transfected with HNRNPC shRNA plasmids (Shanghai Genechem Co., Shanghai, China) and the lentivirus packaging plasmids psPAX2 and pmd2G using

TABLE 1 Comparison of the clinical characteristics between the low and high HNRNPC.

Variable	N of case	HNRNPC		P
		Low	High	
Sample	150	75	75	
Age(year)				0.012
≤60	91	38	53	
>60	59	37	22	
Gender				0.533
Male	139	71	68	
Female	11	4	7	
Tumor stage				0.971
T1	42	21	21	
T2	46	24	22	
T3	35	18	17	
T4	25	11	14	
Unknown	2	1	1	
Clinical stage				0.081
I	23	16	7	
II	25	15	10	
III	32	13	19	
IV	66	28	38	
Unknown	4	3	1	
Distant metastasis				0.316
Yes	1	0	1	
No	149	75	74	
Lymph node metastasis				0.033
Yes	81	34	47	
No	69	41	28	
Survival state				0.02
Alive	90	52	38	
Dead	60	23	37	

Bold values: P<0.05.

jetPRIME (Polyplus transfection Inc, Illkirch, France). At 6-h post transfection, the medium was replaced with DMEM (high glucose) containing 10% FBS. 48-h after transfection, viral particles were collected, and polybrene (8 µg/mL) was applied to assist in the infection of cells, from which GFP⁺ cells were obtained by flow cytometry. The RNAi Consortium (TRC) IDs for the shRNAs are: shHNRNPC-1: 5'-GCCTTCGTTTCAGTATGTTAAT-3' and shHNRNPC-2: 5'-GCGCTTGTCTAAGATCAAATT-3'. Scrambled shRNA was used as the negative control.

RNA extraction and quantitative real-time PCR

Cellular RNA was extracted with TRIzolTM reagent (Invitrogen) and reverse-transcribed to complementary DNA (cDNA) using the High-Capacity cDNA Reverse Transcription Kit (Invitrogen). Quantitative PCR was carried out with the ABI StepOneTM Real-Time PCR system (Applied Biosystems) using SYBR[®] Green Realtime PCR Master Mix (Toyobo). Relative gene expression was calculated using the $2^{-\Delta\Delta C_t}$ method. Primers were synthesized by Sangon Biotech (Shanghai, China): HNRNPC forward 5'-GTTACCAACAAGACAGATCCTCG-3' and reverse 5'-AGGCAAAGCCCTTATGAACAG-3'; and GAPDH forward 5'-CAGGAGGCATTGCTGATGAT-3' and reverse 5'-GAAGGCTGGGGCTCATT-3'.

Protein extraction and western blot

Cells were washed three times with PBS and lysed in RIPA (Beyotime, Guangzhou, China) buffer containing PMSF. Protein concentrations were quantitated using the BCA Protein Assay Kit (Beyotime, Guangzhou, China). Protein samples were separated by 8% or 10% SDS-PAGE and transferred to PVDF membrane (Millipore, Billerica, MA, USA). After blocking with 5% non-fat milk, the membranes were incubated overnight at 4°C with primary antibodies, followed by incubation with a secondary antibody at room temperature. The primary antibodies used were anti-hnRNPC (Abcam, ab133607, 1:1000) and anti-β-actin (Cell Signaling Technology, 3700, 1:1000). Protein-antibody complexes were detected with enhanced chemiluminescence (ECL) reagent (Bio-Rad, Hercules, CA) using the ChemiDocTM XRS imaging system (Bio-Rad, USA).

Immunohistochemistry

The patient tissues were fixed overnight with 10% (vol/vol) neutral-buffered formalin and embedded in paraffin. Sections of 5 µm thickness were then prepared. These sections were deparaffinized, rehydrated in xylene, and treated with graded ethanol concentrations. Endogenous peroxidase activity was quenched using 3% hydrogen peroxide, and antigen retrieval was carried out with an EDTA buffer. The sections were incubated overnight in a humid chamber at 4°C with the primary antibodies. After a 1-hour incubation with secondary antibodies at room temperature, the 3, 3'-diaminobenzidine (ZSGB-BIO, Beijing, China) detection system was used to visualize the staining. Stained tissue sections were observed using a light microscope (Nikon, Tokyo, Japan) and quantitatively scored based on the percentage of positive cells and staining intensity. The H-score was assessed using the following formula: (percentage of weak

intensity $\times 1$) + (percentage of moderate intensity $\times 2$) + (percentage of strong intensity $\times 3$).

Cell proliferation assay

Cells were seeded on 96-well plates at a density of 1000 cells per well and incubated at 37°C, 5% CO₂. The absorbance was measured on days 1, 2, and 3 at a wavelength of 450 nm (A₄₅₀) using a microplate reader (Bio-Rad), after which CCK8 (Dojindo, Tokyo, Japan) was added and the cells were incubated for 3 h at 37°C. Cell proliferation was quantitated by measuring the relative cell viability.

Cell apoptosis assay

Cells on 6-well plates were trypsinized, washed twice with cold PBS, and resuspended in 500 μ L Annexin V binding buffer. After incubation with Annexin V-FITC and PI in the dark for 15 min, the cells were analyzed by flow cytometry, and the apoptotic population was measured using the FlowJo X software.

Wound healing assay

Cells were seeded on 6-well plates at a density of 5×10^5 cells/well, and at 90% confluence were scratched with a sterile pipette tip. After washing with culture medium to remove debris, cells were allowed to migrate for 48 h. The wounds were photographed at 0 h and 48 h using an Olympus IX53 inverted phase contrast microscope (Olympus, Tokyo, Japan). Three random fields were marked and measured. The migration index is expressed as the percentage of wound remaining at 48 h relative to that at 0 h.

Migration and Matrigel[®] invasion assay

Cells were resuspended in serum-free DMEM at a density of 5×10^4 cells/mL. 200 μ L diluted cells were seeded onto the upper compartment of Transwell[®] chambers (8.0- μ m pore size, Corning) or Matrigel[®] (5 \times dilution, 50 μ L, BD Bioscience), and 600 μ L DMEM supplemented with 10% FBS was added to the lower compartment. After a 48-h incubation, the migrating/invading cells were fixed with 4% paraformaldehyde, stained with 0.1% crystal violet, photographed under a microscope, and then counted using the ImageJ software.

RNA sequencing

SeqHealth Tech Co., Ltd. (Wuhan, China) conducted RNA extraction, library preparation, and high-throughput sequencing data analysis. The KCTM Stranded mRNA Library Prep Kit for Illumina[®] (Wuhan Seqhealth Co., Ltd. China) was employed to prepare the RNA library, and 2 μ g RNA per sample was used as input material. The library products corresponding to 200–500 bps were enriched,

quantitated, and then sequenced and analyzed on the DNBSEQ-T7 sequencer (MGI Tech Co., Ltd. China) with the PE150 model. Gene Ontology (GO) enrichment analysis was performed using the KOBAS software (version: 2.1.1) to determine the biological implications of the differentially expressed genes (DEGs).

Methylated RNA immunoprecipitation sequencing

MeRIP-seq data analysis was conducted by SeqHealth Tech Co., Ltd. (Wuhan, China). Total RNA was extracted by TRIzol[™] reagent (Invitrogen), and contaminating DNA was digested with DNase I. A 50- μ g aliquot of total RNA was subjected to polyadenylated RNA enrichment by VAHTS[®] mRNA Capture Beads, and 20 mM ZnCl₂ was used to shear the mRNA into approximately 100–200-nt fragments, which were then subjected to immunoprecipitation (IP) with an anti-m6A antibody (Synaptic Systems). The KC-Digital[™] Stranded mRNA Library Prep Kit for Illumina[®] (Wuhan SeqHealth Co., Ltd. China) was used to construct the stranded RNA sequencing library. The library products were enriched, quantitated, and then sequenced and analyzed. GO and Kyoto Encyclopedia of Genes and Genomes (KEGG) enrichment analyses were performed to determine the biological implications of the DEGs.

Signature construction

A univariate COX proportional hazards regression analysis was performed to determine the prognostic value of m6A-related genes. Subsequently, a stepwise COX proportional hazards regression model was used to filter out the most predictive genes among the survival-related candidate markers (Supplementary Table S1). Four genes and their coefficients were chosen with the minimum criteria, and the risk score for the signature was calculated using the following formula:

$$\text{Risk score} = \text{Coef}_1 * x_1 + \text{Coef}_2 * x_2 + \dots + \text{Coef}_n * x_n$$

where Coef_n and x_n are the coefficient and the z -score-transformed relative expression value for every chosen gene, respectively. Finally, HNSCC patients were divided into high- and low-risk groups according to the median risk score.

Mouse xenograft model

All animal experiments were approved by the Animal Ethics Committee of the Zhengzhou Cancer Institute in Henan. Female BALB/c-nu/nu mice (6–8 weeks old) were bred at Zhengzhou Cancer Institute (Henan, China) and housed under specific pathogen-free (SPF) conditions in a laboratory animal facility. A total of 3.5×10^5 wild-type CAL-27 and HSC-3 cells or those stably expressing shHNRNPC were subcutaneously injected into the right dorsal flank of the mice (5 per group). The mice weight and tumor size were measured once every three days. After 25 days, the mice were sacrificed, and the tumors were harvested at necropsy for further analysis.

Statistical analysis

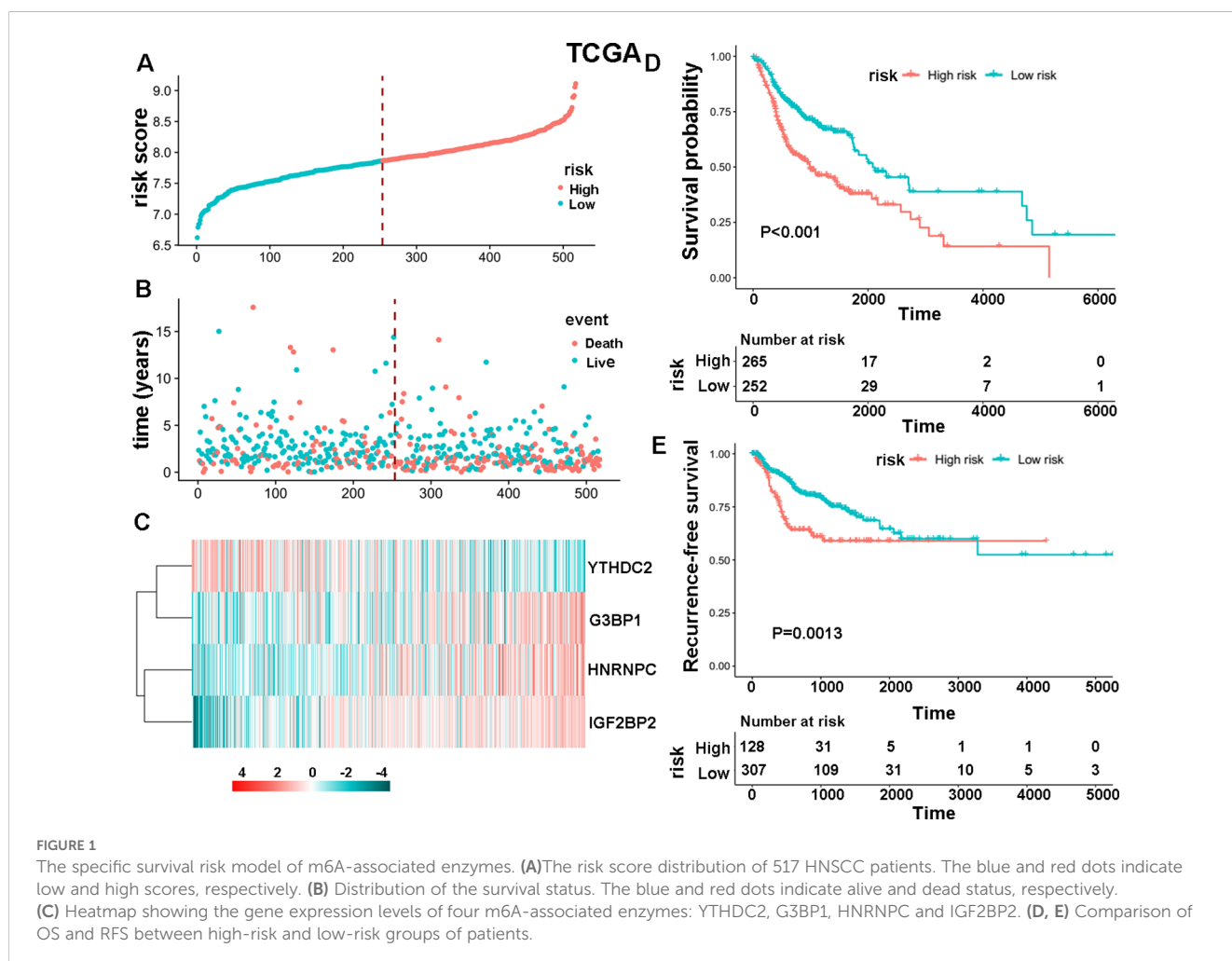
Pearson correlation analysis was performed to assess the association between two regulators. Kaplan–Meier curves were used to compare the OS or recurrence-free survival (RFS) rates of patients between the high- and low-risk groups, and the survival distributions in the two groups was evaluated by the log-rank test. The clinical characteristics were compared using the chi-square test. While differences between groups were compared using a Student’s *t*-test. Statistical analyses were performed using the R software version 3.6.1 (<https://www.r-project.org>), IBM SPSS Statistics V21.0 (IBM SPSS Inc., Chicago, USA), or GraphPad Prism 7.0 (GraphPad, San Diego, CA, USA). *P* < 0.05 was considered statistically significant.

Results

Establishment of the specific survival risk model of m6A-associated enzymes

The study initially analyzed the expression levels of 30 m6A regulators in 504 HNSCC samples and 44 normal tissues from the

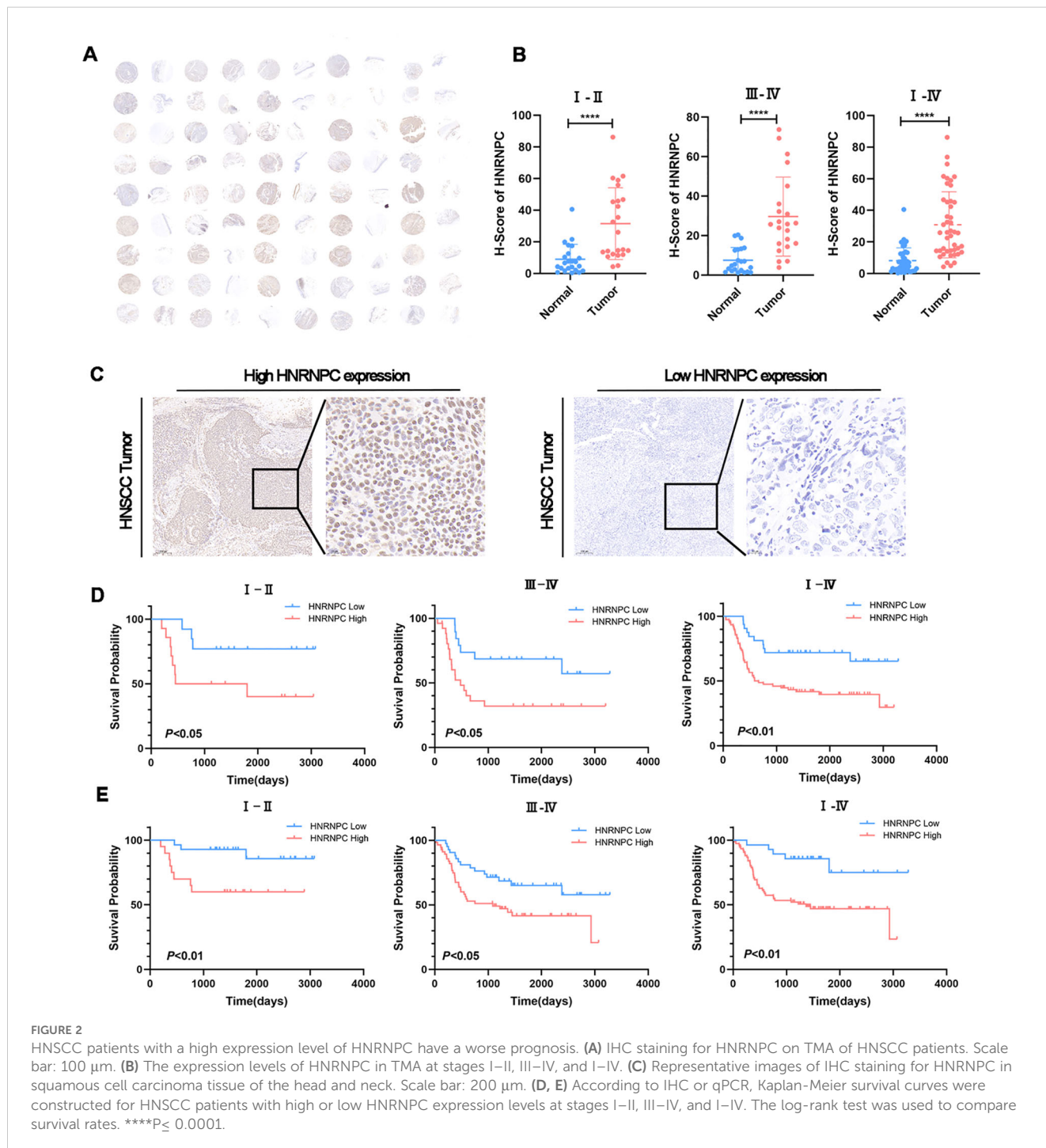
TCGA database, finding that 28 genes were upregulated and two were not significantly different (Supplementary Figure S1). Subsequently, data from 517 HNSCC patients was used to develop a specific survival risk model based on m6A-associated enzymes’ gene expression. This model identified a high-risk group of 265 patients and a low-risk group of 252 patients (Figure 1A). The survival status of these patients is shown in Figure 1B. Results of survival analysis based on these four m6A-associated proteins (Figure 1C) show that the HNSCC patients in the high-risk group had a significantly shorter OS (Figure 1D, *P* < 0.001) and recurrence-free survival (RFS) (Figure 1E, *P* = 0.0013) than those in the low-risk group. We further evaluated the survival status of both the high-risk and low-risk groups according to several clinicopathological parameters including clinical stage, status of lymph node metastasis, and gender. The results demonstrate that the high-risk patients had a poorer prognosis than the low-risk patients (Supplementary Figure S2). These findings were validated in an independent dataset from the GEO database, confirming the stability and reliability of the m6A-associated survival risk model. (Supplementary Figures S3A–E). Additionally, it was noted that *HNRNPC* showed the highest expression levels among the four selected genes in both HNSCC and paired normal tissues (Supplementary Figure S3F).



HNSCC patients with high expression levels of *HNRNPC* have a worse prognosis

The tissue microarray (TMA) immunohistochemistry (IHC) results revealed significantly higher *HNRNPC* expression in HNSCC tissues compared to adjacent normal tissues (Figures 2A, B, $P < 0.0001$). Additionally, 150 tumor samples were collected from HNSCC patients. We further compared the clinical characteristics between patient groups with high and low

HNRNPC expression levels and observed statistically significant differences in tumor stage, lymph node metastasis, and survival state. However, no significant differences were detected among the other clinical features (Table 1). The patients were then categorized into high and low expression groups based on the results of IHC (Figure 2C) and qPCR. Notably, patients with high *HNRNPC* expression in stages I-II, III-IV, and I-IV showed a lower survival probability in comparison with those with low expression (Figures 2D, E).



Repression of *HNRNPC* arrests malicious biological behavior of CAL-27 and HSC-3 cells

Our study focused on the potential function of *HNRNPC* in HNSCC cells. The expression of *HNRNPC* in HSC-3 and CAL-27 cells was silenced by shRNA and verified at the protein and mRNA levels (Figures 3A, B). Knockdown of *HNRNPC* significantly reduced the cell proliferation rate at both 48 h and 72 h (Figure 3C, $P < 0.001$) and promoted apoptosis (Figures 3D, E). A larger wound area (Figures 4A, B) and a significantly reduced invasive ability (Figures 4C, D) were found following *HNRNPC* knockdown, strongly implying that *HNRNPC* plays a crucial role in the migration and invasion of CAL-27 and HSC-3 cells.

HNRNPC is associated with cell differentiation, cell migration, cell cycle, cell proliferation, and apoptosis

We knocked down *HNRNPC* in HSC-3 and CAL-27 cells and then performed RNA-seq. GO analysis identified that the differentially expressed genes (DEGs) were enriched in cell differentiation, cell migration, cell cycle, angiogenesis, extracellular matrix organization, cell proliferation, and T cell-mediated cytotoxicity (Figures 5A, B). DEGs involved in apoptosis, migration, and invasion are shown in the heatmap (Figures 5C, D). MeRIP-seq and conventional RNA-seq were combined to screen the DEGs in CAL-27 cells following knockdown of *HNRNPC* (Figure 5E). Results of KEGG analysis

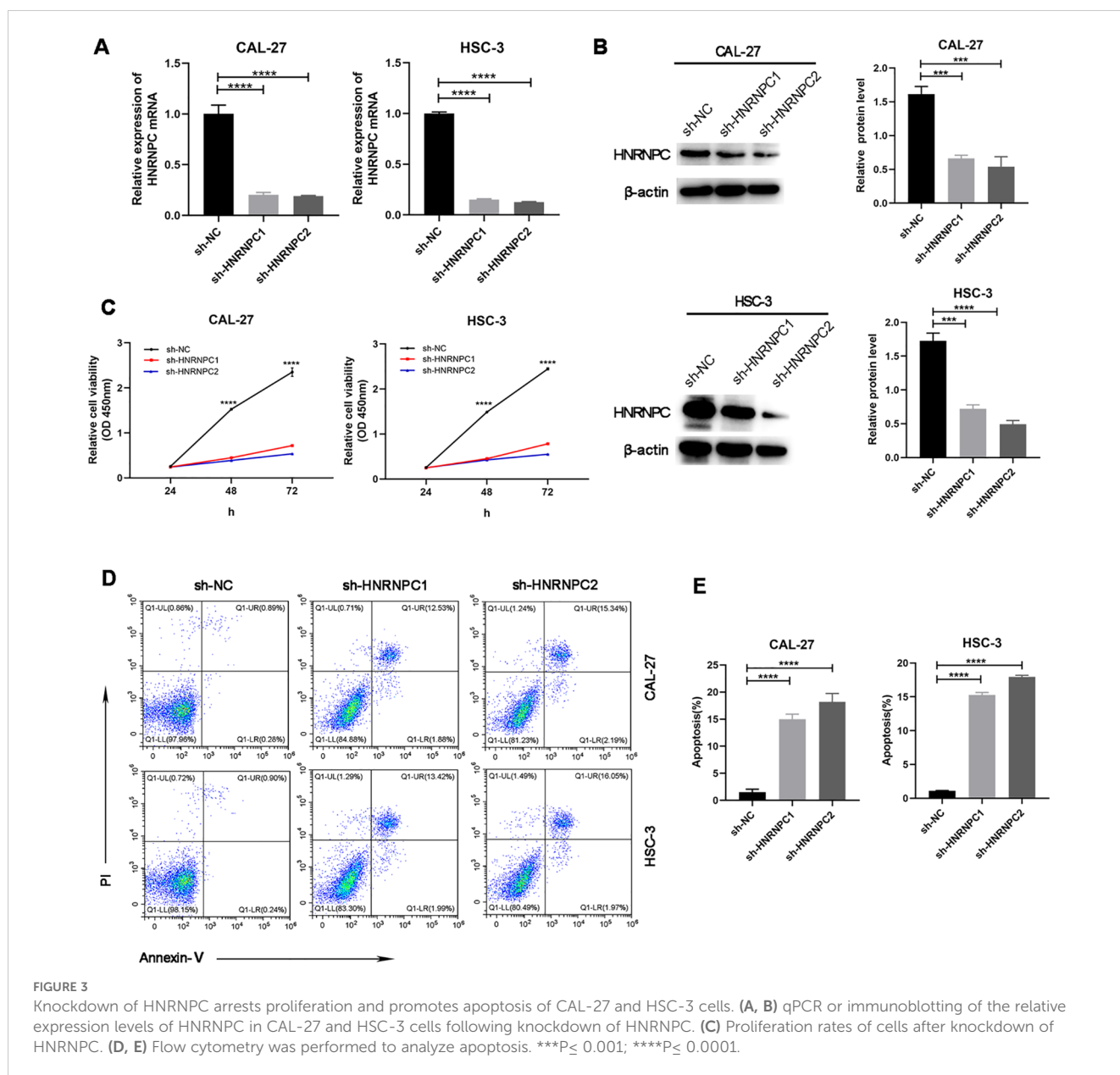


FIGURE 3

Knockdown of *HNRNPC* arrests proliferation and promotes apoptosis of CAL-27 and HSC-3 cells. (A, B) qPCR or immunoblotting of the relative expression levels of *HNRNPC* in CAL-27 and HSC-3 cells following knockdown of *HNRNPC*. (C) Proliferation rates of cells after knockdown of *HNRNPC*. (D, E) Flow cytometry was performed to analyze apoptosis. *** $P \leq 0.001$; **** $P \leq 0.0001$.

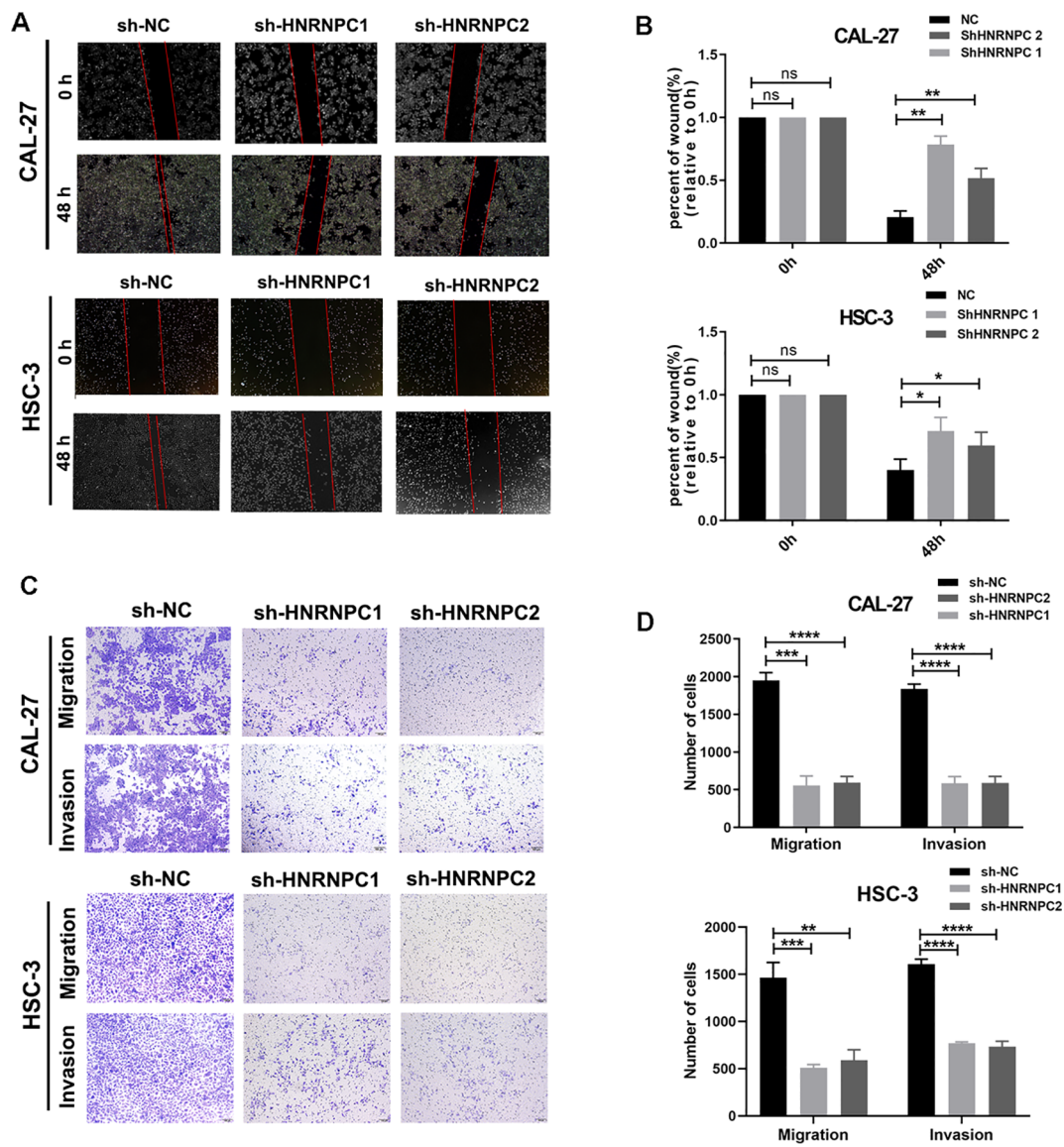


FIGURE 4 Knockdown of HNRNPC decreases the migratory and invasive abilities of CAL-27 and HSC-3 cells. (A) Images of the wound healing assay. (B) Wound area (relative to 0 h) was measured and analyzed. (C) Images of the migration and invasion assay. (D) The number of cells that migrated and invaded was recorded and analyzed. * $P \leq 0.05$; ** $P \leq 0.01$; *** $P \leq 0.001$; **** $P \leq 0.0001$; ns $P > 0.05$.

show that the DEGs were associated with tumor development processes, such as apoptosis and the cell cycle (Figure 5F), and GO analysis data demonstrate enrichment in apoptosis, cell differentiation, cell division, and the cell cycle (Figure 5G).

HNRNPC promotes xenograft HNSCC tumor growth *in vivo*

To assess whether *HNRNPC* impacts tumorigenesis *in vivo*, a xenograft tumor model was established via subcutaneous injection of CAL-27-NC, CAL-27-shHNRNPC, HSC-3-NC, or HSC-3-shHNRNPC cells into the right dorsal flank of mice. After a period of 25 days, the mice were sacrificed and the tumors were surgically removed (Figure 6A). The tumor volume in the

HNRNPC-knockdown groups was significantly lower (100 mm³ CAL-27 and 200 mm³ HSC-3) than that in the control groups (250 mm³ CAL-27 and 500 mm³ HSC-3) ($P < 0.05$) (Figures 6B, C).

Discussion

The initiation and development of HNSCC is a multistep process that involves gradual acquisition of genetic and epigenetic alterations, leading to uncontrolled growth and proliferation of tumor cells (20). m6A methylation is the most abundant mRNA and long noncoding RNA (lncRNA) modification in mammals, occurring at the sixth N position of adenosine and being dynamic and reversible (21). Increasing evidence suggests that m6A methylation plays a critical role in malignant tumors. Aberrant

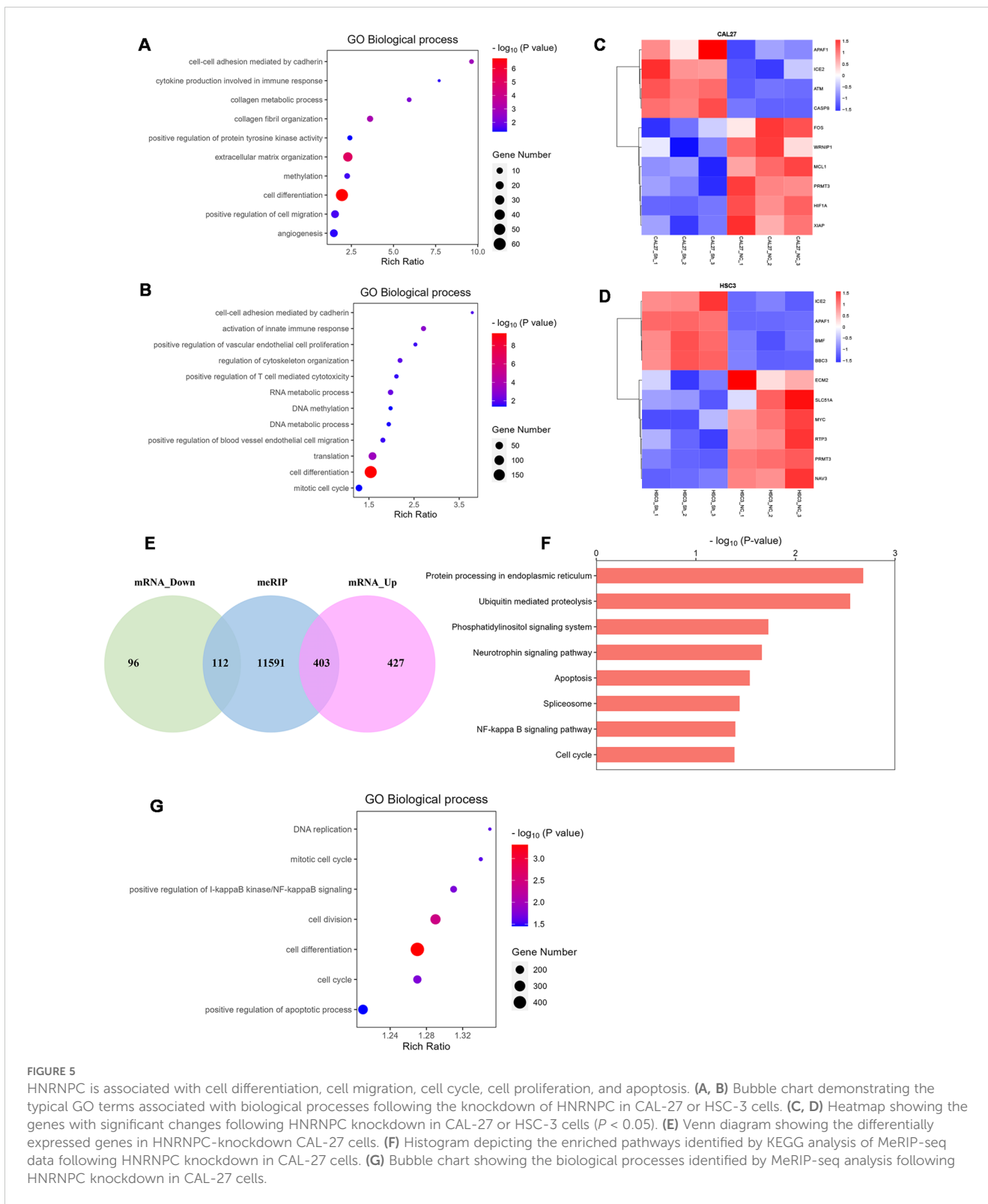
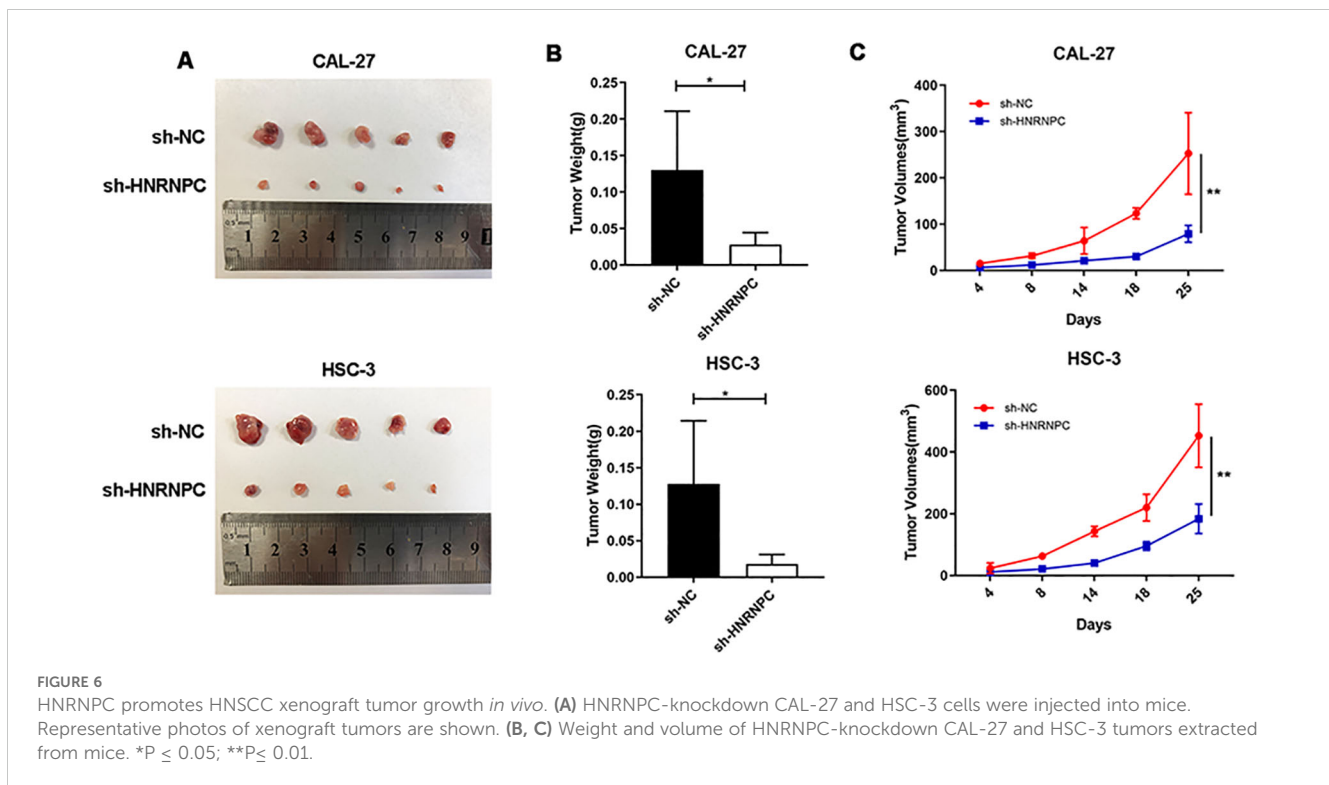


FIGURE 5

HNRNPC is associated with cell differentiation, cell migration, cell cycle, cell proliferation, and apoptosis. (A, B) Bubble chart demonstrating the typical GO terms associated with biological processes following the knockdown of HNRNPC in CAL-27 or HSC-3 cells. (C, D) Heatmap showing the genes with significant changes following HNRNPC knockdown in CAL-27 or HSC-3 cells ($P < 0.05$). (E) Venn diagram showing the differentially expressed genes in HNRNPC-knockdown CAL-27 cells. (F) Histogram depicting the enriched pathways identified by KEGG analysis of MeRIP-seq data following HNRNPC knockdown in CAL-27 cells. (G) Bubble chart showing the biological processes identified by MeRIP-seq analysis following HNRNPC knockdown in CAL-27 cells.

m6A RNA methylation modifications have been demonstrated to facilitate carcinogenesis and the progression of many tumor types, such as bladder cancer (22), ovarian cancer (23), and hepatocellular carcinoma (24), in addition to contributing to the formation of the tumor microenvironment and poor prognosis in gastric (25), and lung cancer (26). Herein, m6A-related genes were extracted from

the TCGA database and a risk score was constructed using a univariate and stepwise COX proportional hazards regression analysis. The risk score indicates that four genes, *YTHDC2*, *HNRNPC*, *IGF2BP2* and *G3BP1*, were associated with poor OS and RFS of HNSCC patients. Moreover, the risk score demonstrates a significant association with clinical parameters involved in tumor



stage, lymph node metastasis and gender, which was further verified using GEO data. Consistent with the findings of this study, univariate Cox regression analyses of TCGA-HNSCC cohort data from three independent studies indicate that the expression of several m6A regulators is linked to clinical outcomes, including overall survival in HNSCC patients (27–29). Cai et al. found a strong positive correlation between m6A regulator expression and HNSCC progression. Their forest plot analysis of Cox regression data identified m6A readers, such as *IGF2BP1*, *IGF2BP2*, and *HNRNPC*, as factors associated with poor prognosis (29). Among the four genes selected in this study, *YTHDC2*, as a member of the YTH protein family, can recognize m6A-binding mRNA in the nucleus, improving translation efficiency and reducing mRNA abundance (30). Knockout of *YTHDC2* weakens the expression of metastasis-related genes, such as hypoxia-inducible factor-1 alpha (*HIF-1α*) and *twist1*, thereby inhibiting the metastasis of colon tumor cells (31). The prognosis is favorable for patients with downregulated *YTHDC2* expression in HNSCC (32). *IGF2BP2* is a member of the insulin-like growth factor-2 binding protein family, which promotes more stable mRNA translation in an m6A-dependent manner (11). *IGF2BP2* overexpression promotes pancreatic ductal adenocarcinoma progression by binding to and stabilizing glucose transporter 1 (*GLUT1*) mRNA (33). Analysis of the TCGA database and IHC demonstrate that *IGF2BP2* is overexpressed in HNSCC patients with a poor prognosis (34). *G3BP1* is a member of the Ras-GTPase-activating protein binding protein family and plays an important role in RNA metabolism (35). Knockdown of *G3BP1* inhibits the G0/G1 phase of the cell cycle and reduces cell proliferation, migration, and invasion by inactivating the PI3K/AKT/mTOR and Wnt signaling pathways in esophageal carcinoma (36). *G3BP1* promotes renal cell carcinoma

by connecting IL-6 and STAT3 signal transduction, and increases CD4⁺ T cell infiltration during the progression and metastasis of oral squamous cell carcinoma (OSCC) (37).

Among the four selected genes, *HNRNPC* had the highest expression in both tumor and normal tissues in the TCGA database. Our findings indicate that *HNRNPC* is highly expressed in tumor tissues compared to adjacent normal tissues, aligning with previous studies that suggest a tumorigenic role for *HNRNPC* in HNSCC (38). However, further *in vitro* and *in vivo* investigation is required to harvest more accurate functional information for *HNRNPC* in HNSCC. Here, knockdown of *HNRNPC* significantly inhibited cell proliferation and promoted cell apoptosis *in vitro*, in addition to impairing tumorigenesis in the mouse model. Moreover, RNA-seq and MeRIP-seq data demonstrate that *HNRNPC* is involved in cell differentiation, cell migration, cell cycle, cell proliferation, and apoptosis. These findings demonstrate that *HNRNPC* plays a critical role in HNSCC tumorigenesis. To date, several studies have focused on the role of *HNRNPC* in tumorigenesis and development. An increasing number of reports demonstrate that *HNRNPC* plays distinct roles in the metastasis and invasion of different cancers; for instance, elevated levels of *HNRNPC* are essential for the proliferative ability of two breast cancer cell lines (39). Wang et al. found that *HNRNPC* expression was elevated in glioma tissues compared to normal brain tissues, and higher levels of *HNRNPC* were associated with advanced clinical stages (40). Furthermore, overexpression of *HNRNPC* promotes OSCC progression via epithelial–mesenchymal transition (EMT) (41), in addition to chemoresistance in gastric cancer with poor OS and free of progression (FP) (42).

Although the present study has important clinical significance, several limitations still need to be considered. To gain a

comprehensive understanding of the molecular landscape of HNSCC and further refine the risk score model, it is essential to investigate the underlying mechanisms involving *HNRNPC*. Additionally, further studies are warranted to investigate the function and underlying mechanisms of the remaining three identified m6A biomarkers.

Conclusions

The present study demonstrates that *HNRNPC* is involved in the development of HNSCC and patient prognosis. Knockdown of *HNRNPC* can inhibit proliferation and metastasis and promote apoptosis of HNSCC cells. *HNRNPC* may become a new biomarker for predicting the prognosis of HNSCC patients, providing new insights and tools for treatment.

Data availability statement

The original contributions presented in the study are included in the article/[Supplementary Material](#). Further inquiries can be directed to the corresponding author/s.

Ethics statement

The studies involving humans were approved by the Ethics Committee of the First Affiliated Hospital of Zhengzhou University. The studies were conducted in accordance with the local legislation and institutional requirements. The ethics committee/institutional review board waived the requirement of written informed consent for participation from the participants or the participants' legal guardians/next of kin because Informed consent was waived due to the retrospective nature of tissue sample collection from patients diagnosed with HNSCC. Additionally, there exist no personal privacy or commercial interests. The animal study was approved by the Ethics Committee of the First Affiliated Hospital of Zhengzhou University. The study was conducted in accordance with the local legislation and institutional requirements.

Author contributions

YIZ: Conceptualization, Data curation, Formal Analysis, Funding acquisition, Investigation, Methodology, Project administration, Resources, Software, Supervision, Validation, Visualization, Writing – original draft, Writing – review & editing. YW: Conceptualization, Data curation, Formal Analysis, Funding acquisition, Investigation, Methodology, Project administration, Resources, Software, Supervision, Validation, Visualization, Writing – original draft, Writing – review & editing. JP: Conceptualization, Data curation, Formal Analysis, Funding acquisition, Investigation, Methodology, Project administration, Resources, Software, Supervision, Validation,

Visualization, Writing – review & editing. KZ: Conceptualization, Data curation, Investigation, Methodology, Software, Supervision, Writing – review & editing. LL: Conceptualization, Data curation, Formal Analysis, Writing – review & editing. YaZ: Data curation, Methodology, Writing – review & editing. ZZ: Methodology, Writing – review & editing. SY: Methodology, Writing – review & editing. SL: Conceptualization, Data curation, Investigation, Software, Visualization, Writing – review & editing. FY: Conceptualization, Data curation, Formal Analysis, Funding acquisition, Investigation, Methodology, Project administration, Resources, Software, Supervision, Validation, Visualization, Writing – review & editing. LW: Conceptualization, Data curation, Formal Analysis, Funding acquisition, Investigation, Methodology, Project administration, Resources, Software, Supervision, Validation, Visualization, Writing – original draft, Writing – review & editing.

Funding

The author(s) declare that financial support was received for the research, authorship, and/or publication of this article. This research was supported by grants from the National Natural Science Foundation of China (82002876) and Technique Foundation for youth of Henan (SBGJ202103062).

Conflict of interest

The authors declare that the research was conducted in the absence of any commercial or financial relationships that could be construed as a potential conflict of interest.

Generative AI statement

The author(s) declare that no Generative AI was used in the creation of this manuscript.

Publisher's note

All claims expressed in this article are solely those of the authors and do not necessarily represent those of their affiliated organizations, or those of the publisher, the editors and the reviewers. Any product that may be evaluated in this article, or claim that may be made by its manufacturer, is not guaranteed or endorsed by the publisher.

Supplementary material

The Supplementary Material for this article can be found online at: <https://www.frontiersin.org/articles/10.3389/fonc.2025.1516867/full#supplementary-material>

References

- Forastiere A, Koch W, Trotti A, Sidransky D. Head and neck cancer. *N Engl J Med.* (2001) 345:1890–900. doi: 10.1056/NEJMra001375
- Sanderson RJ, Ironside JA. Squamous cell carcinomas of the head and neck. *BMJ.* (2002) 325:822–7. doi: 10.1136/bmj.325.7368.822
- Ludwig ML, Birkeland AC, Hoesli R, Swicicki P, Spector ME, Brenner JC. Changing the paradigm: the potential for targeted therapy in laryngeal squamous cell carcinoma. *Cancer Biol Med.* (2016) 13:87–100. doi: 10.20892/j.issn.2095-3941.2016.0010
- He L, Li H, Wu A, Peng Y, Shu G, Yin G. Functions of N6-methyladenosine and its role in cancer. *Mol Cancer.* (2019) 18:176. doi: 10.1186/s12943-019-1109-9
- Jia G, Fu Y, He C. Reversible RNA adenosine methylation in biological regulation. *Trends Genet.* (2013) 29:108–15. doi: 10.1016/j.tig.2012.11.003
- Liu J, Yue Y, Han D, Wang X, Fu Y, Zhang L, et al. A METTL3-METTL14 complex mediates mammalian nuclear RNA N6-adenosine methylation. *Nat Chem Biol.* (2014) 10:93–5. doi: 10.1038/nchembio.1432
- Jia G, Fu Y, Zhao X, Dai Q, Zheng G, Yang Y, et al. N6-methyladenosine in nuclear RNA is a major substrate of the obesity-associated FTO. *Nat Chem Biol.* (2011) 7:885–7. doi: 10.1038/nchembio.687
- Li A, Chen YS, Ping XL, Yang X, Xiao W, Yang Y, et al. Cytoplasmic m(6)A reader YTHDF3 promotes mRNA translation. *Cell Res.* (2017) 27:444–7. doi: 10.1038/cr.2017.10
- Ma S, Chen C, Ji X, Liu J, Zhou Q, Wang G, et al. The interplay between m6A RNA methylation and noncoding RNA in cancer. *J Hematol Oncol.* (2019) 12:121. doi: 10.1186/s13045-019-0805-7
- König J, Zarnack K, Rot G, Curk T, Kayıkcı M, Zupan B, et al. iCLIP reveals the function of hnRNP particles in splicing at individual nucleotide resolution. *Nat Struct Mol Biol.* (2010) 17:909–15. doi: 10.1038/nsmb.1838
- Huang H, Weng H, Sun W, Qin X, Shi H, Wu H, et al. Recognition of RNA N(6)-methyladenosine by IGF2BP proteins enhances mRNA stability and translation. *Nat Cell Biol.* (2018) 20:285–95. doi: 10.1038/s41556-018-0045-z
- Zarnack K, König J, Tajnik M, Martincorena I, Eustermann S, Stévant I, et al. Direct competition between hnRNP C and U2AF65 protects the transcriptome from the exonization of Alu elements. *Cell.* (2013) 152:453–66. doi: 10.1016/j.cell.2012.12.023
- McCloskey A, Taniguchi I, Shinmyozu K, Ohno M. hnRNP C tetramer measures RNA length to classify RNA polymerase II transcripts for export. *Science.* (2012) 335:1643–6. doi: 10.1126/science.1218469
- Velusamy T, Shetty P, Bhandary YP, Liu MC, Shetty S. Posttranscriptional regulation of urokinase receptor expression by heterogeneous nuclear ribonucleic protein C. *Biochemistry.* (2008) 47:6508–17. doi: 10.1021/bi702338y
- Gruber AJ, Schmidt R, Gruber AR, Martin G, Ghosh S, Belmadani M, et al. A comprehensive analysis of 3' end sequencing data sets reveals novel polyadenylation signals and the repressive role of heterogeneous ribonucleoprotein C on cleavage and polyadenylation. *Genome Res.* (2016) 26:1145–59. doi: 10.1101/gr.202432.115
- Lee EK, Kim HH, Kuwano Y, Abdelmohsen K, Srikantan S, Subaran SS, et al. hnRNP C promotes APP translation by competing with FMRP for APP mRNA recruitment to P bodies. *Nat Struct Mol Biol.* (2010) 17:732–9. doi: 10.1038/nsmb.1815
- Park YM, Hwang SJ, Masuda K, Choi KM, Jeong MR, Nam DH, et al. Heterogeneous nuclear ribonucleoprotein C1/C2 controls the metastatic potential of glioblastoma by regulating PDCD4. *Mol Cell Biol.* (2012) 32:4237–44. doi: 10.1128/MCB.00443-12
- Liu J, Sun G, Pan S, Qin M, Ouyang R, Li Z, et al. The Cancer Genome Atlas (TCGA) based m(6)A methylation-related genes predict prognosis in hepatocellular carcinoma. *Bioengineered.* (2020) 11:759–68. doi: 10.1080/21655979.2020.1787764
- Sarbanes SL, Le Pen J, Rice CM. Friend and foe, HNRNPC takes on immunostimulatory RNAs in breast cancer cells. *EMBO J.* (2018) 37(23):e100923. doi: 10.15252/embj.2018100923
- Johnson DE, Burtness B, Leemans CR, Lui VWY, Bauman JE, Grandis JR. Head and neck squamous cell carcinoma. *Nat Rev Dis Primers.* (2020) 6:92. doi: 10.1038/s41572-020-00224-3
- Gonzales-van-Horn SR, Sarnow P. Making the mark: the role of adenosine modifications in the life cycle of RNA viruses. *Cell Host Microbe.* (2017) 21:661–9. doi: 10.1016/j.chom.2017.05.008
- Han J, Wang JZ, Yang X, Yu H, Zhou R, Lu HC, et al. METTL3 promote tumor proliferation of bladder cancer by accelerating pri-miR221/222 maturation in m6A-dependent manner. *Mol Cancer.* (2019) 18:110. doi: 10.1186/s12943-019-1036-9
- Liu T, Wei Q, Jin J, Luo Q, Liu Y, Yang Y, et al. The m6A reader YTHDF1 promotes ovarian cancer progression via augmenting EIF3C translation. *Nucleic Acids Res.* (2020) 48:3816–31. doi: 10.1093/nar/gkaa048
- Chen Y, Peng C, Chen J, Chen D, Yang B, He B, et al. WTAP facilitates progression of hepatocellular carcinoma via m6A-HuR-dependent epigenetic silencing of ETS1. *Mol Cancer.* (2019) 18:127. doi: 10.1186/s12943-019-1053-8
- Zhang B, Wu Q, Li B, Wang D, Wang L, Zhou YL. m(6)A regulator-mediated methylation modification patterns and tumor microenvironment infiltration characterization in gastric cancer. *Mol Cancer.* (2020) 19:53. doi: 10.1186/s12943-020-01170-0
- Li Y, Gu J, Xu F, Zhu Q, Chen Y, Ge D, et al. Molecular characterization, biological function, tumor microenvironment association and clinical significance of m6A regulators in lung adenocarcinoma. *Brief Bioinform.* (2021) 22(4):bbaa225. doi: 10.1093/bib/bbaa225
- Chen Y, Jiang X, Li X, Yan D, Liu J, Yang J, et al. The methylation modification of m6A regulators contributes to the prognosis of head and neck squamous cell carcinoma. *Ann Transl Med.* (2021) 9:1346. doi: 10.21037/atm-21-4077
- Zhai Y, Zheng L. m6A RNA methylation regulator-related signatures exhibit good prognosis prediction ability for head and neck squamous cell carcinoma. *Sci Rep.* (2022) 12:16358. doi: 10.1038/s41598-022-20873-6
- Cai H, Liang J, Jiang Y, Tan R, Hou C, Hou J. Integrative analysis of N6-methyladenosine-related enhancer RNAs identifies distinct prognosis and tumor immune micro-environment patterns in head and neck squamous cell carcinoma. *Cancers (Basel).* (2022) 14(19):4657. doi: 10.3390/cancers14194657
- Hsu PJ, Zhu Y, Ma H, Guo Y, Shi X, Liu Y, et al. Ythdc2 is an N(6)-methyladenosine binding protein that regulates mammalian spermatogenesis. *Cell Res.* (2017) 27:1115–27. doi: 10.1038/cr.2017.99
- Tanabe A, Tanikawa K, Tsunetomi M, Takai K, Ikeda H, Konno J, et al. RNA helicase YTHDC2 promotes cancer metastasis via the enhancement of the efficiency by which HIF-1 α mRNA is translated. *Cancer Lett.* (2016) 376:34–42. doi: 10.1016/j.canlet.2016.02.022
- Kasowitz SD, Ma J, Anderson SJ, Leu NA, Xu Y, Gregory BD, et al. Nuclear m6A reader YTHDC1 regulates alternative polyadenylation and splicing during mouse oocyte development. *PLoS Genet.* (2018) 14:e1007412. doi: 10.1371/journal.pgen.1007412
- Huang S, Wu Z, Cheng Y, Wei W, Hao L. Insulin-like growth factor 2 mRNA binding protein 2 promotes aerobic glycolysis and cell proliferation in pancreatic ductal adenocarcinoma via stabilizing GLUT1 mRNA. *Acta Biochim Biophys Sin (Shanghai).* (2019) 51:743–52. doi: 10.1093/abbs/gmz048
- Deng X, Jiang Q, Liu Z, Chen W. Clinical significance of an m6A reader gene, IGF2BP2, in head and neck squamous cell carcinoma. *Front Mol Biosci.* (2020) 7:68. doi: 10.3389/fmolb.2020.00068
- Sahoo PK, Lee SJ, Jaiswal PB, Alber S, Kar AN, Miller-Randolph S, et al. Axonal G3BP1 stress granule protein limits axonal mRNA translation and nerve regeneration. *Nat Commun.* (2018) 9:3358. doi: 10.1038/s41467-018-05647-x
- Zhang LN, Zhao L, Yan XL, Huang YH. Loss of G3BP1 suppresses proliferation, migration, and invasion of esophageal cancer cells via Wnt/ β -catenin and PI3K/AKT signaling pathways. *J Cell Physiol.* (2019) 234:20469–84. doi: 10.1002/jcp.v234.11
- Hu X, Xia K, Xiong H, Su T. G3BP1 may serve as a potential biomarker of proliferation, apoptosis, and prognosis in oral squamous cell carcinoma. *J Oral Pathol Med.* (2021) 50:995–1004. doi: 10.1111/jop.v50.10
- Zhao X, Cui L. Development and validation of a m(6)A RNA methylation regulators-based signature for predicting the prognosis of head and neck squamous cell carcinoma. *Am J Cancer Res.* (2019) 9:2156–69.
- Wu Y, Zhao W, Liu Y, Tan X, Li X, Zou Q, et al. Function of HNRNPC in breast cancer cells by controlling the dsRNA-induced interferon response. *EMBO J.* (2018) 37(23):e99017. doi: 10.15252/embj.201899017
- Wang LC, Chen SH, Shen XL, Li DC, Liu HY, Ji YL, et al. M6A RNA methylation regulator HNRNPC contributes to tumorigenesis and predicts prognosis in glioblastoma multiforme. *Front Oncol.* (2020) 10:536875. doi: 10.3389/fonc.2020.536875
- Huang GZ, Wu QQ, Zheng ZN, Shao TR, Chen YC, Zeng WS, et al. M6A-related bioinformatics analysis reveals that HNRNPC facilitates progression of OSCC via EMT. *Aging (Albany NY).* (2020) 12:11667–84. doi: 10.18632/aging.103333
- Huang H, Han Y, Zhang C, Wu J, Feng J, Qu L, et al. HNRNPC as a candidate biomarker for chemoresistance in gastric cancer. *Tumour Biol.* (2016) 37:3527–34. doi: 10.1007/s13277-015-4144-1